

Age-of-Information With Information Source Diversity in an Energy Harvesting System

Elvina Gindullina¹, Leonardo Badia², *Senior Member, IEEE*, and Deniz Gündüz³, *Senior Member, IEEE*

Abstract—Age of information (AoI) is a key performance metric for the Internet of things (IoT). Timely status updates are essential for many IoT applications; however, they often suffer from harsh energy constraints and the unreliability of underlying information sources. To overcome these unpredictabilities, one can employ multiple sources that track the same process of interest, but with different energy costs and reliabilities. We consider an energy-harvesting (EH) monitoring node equipped with a finite-size battery and collecting status updates from multiple heterogeneous information sources. We investigate the policies that minimize the average AoI, formulating a Markov decision process (MDP) to choose the optimal actions of either updating from one of the sources or remaining idle, based on the current energy level and the AoI at the monitoring node. We analyze the structure of the optimal solution for different cost/AoI distribution combinations, and compare its performance with an aggressive policy that transmits whenever possible.

Index Terms—Age of information, energy harvesting, heterogeneous systems, Internet of Things, Markov decision process.

I. INTRODUCTION

INTERNET OF THINGS (IoT) systems are increasingly being exploited for a variety of applications that encompass every aspect of our lives [2]. In many of these applications freshness of the monitored information can play an important role for the system performance. Age of information (AoI) is a key performance indicator in mission-critical and time-sensitive applications, including smart transportation, healthcare, remote surgery, robotics cooperation, public safety, industrial process automation, to count a few. AoI quantifies the freshness of knowledge about the status of the system being monitored [3], [4]. For instance, in autonomous driving, timely collection of traffic information and vehicle-generated

data is essential for the safety of all road users. Another important example is factory automation, where real-time control of production also requires timely delivery of status updates [5].

One limitation against frequent updates is the energy supply of the sensor. Since sensing devices are typically wireless, and often placed in remote areas, it would be impractical to power them through cables. If the device is powered only through batteries, a significant downtime would hinder the provision of reliable and up-to-date information. In these situations, broad autonomy for reliable IoT systems can be obtained through energy harvesting (EH) combined with rechargeable batteries. This, however, would further require a smart sensing and communication strategy [6]. Indeed, the integration of energy harvesters reduces the maintenance cost of IoT and increases the energy self-sustainability, but comes at a price of not guaranteeing uninterrupted operation of the device.

We focus on an EH monitoring node, whose goal is to track the underlying process as closely as possible, i.e., with the minimum average AoI, within the constraints of stochastic energy arrivals from ambient sources of energy and a finite battery capacity. Also, we consider the role of multiple information sources that monitor the same underlying process of interest called *information source diversity*, where each source provides a different trade-off between the cost of sensing and the freshness of the provided status update. Hence, the policy governing the operation of the system does not simply make a binary choice between providing a new status update or not, but must also include the optimal choice of the specific information source to be used. To clarify, the policy might also choose to wait, instead of updating immediately in a myopic fashion, in order to accumulate energy so as to be able to use a more reliable information source in the future.

We compare the performance of the optimal policy with a greedy “aggressive” update policy in terms of average AoI, highlighting the situations where optimization is really needed as opposed to the simple implementation of an “update whenever needed” strategy. We also quantify the additional gains in the minimal long-term average AoI due to multiple information sources, as well as how the quality of these sources affects the outcome. Finally, we compute the power expenditure of these policies, and discuss how the added dimensionality of the problem affects the system performance.

A. Background

Several papers study the average AoI minimization with a single energy-harvesting source [7]–[19], whereas very

Manuscript received April 23, 2020; revised October 29, 2020, May 5, 2021, and June 8, 2021; accepted June 9, 2021. This work was supported by the European Union’s Horizon 2020 Research and Innovation Programme through the Marie Skłodowska-Curie Grant under Agreement 675891 (SCAVENGE). The work of Deniz Gündüz was supported by the European Research Council (ERC) through Project BEACON under Grant 677854. This article was presented in part at [1]. The editor coordinating the review of this article was H. S. Dhillon. (*Corresponding author: Elvina Gindullina.*)

This work did not involve human subjects or animals in its research.

Elvina Gindullina and Leonardo Badia are with the Department of Information Engineering, University of Padua, 35131 Padua, Italy (e-mail: gindullina@dei.unipd.it; badia@dei.unipd.it).

Deniz Gündüz is with the Department of Electrical and Electronic Engineering, Imperial College London, London SW7 2AZ, U.K. (e-mail: d.gunduz@imperial.ac.uk).

Digital Object Identifier 10.1109/TGCN.2021.3092272

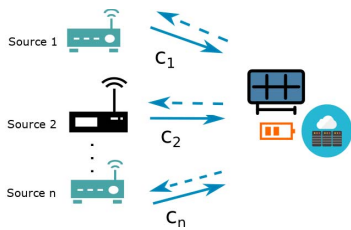


Fig. 1. System model consisting of n information sources.

single IoT device, where an IoT device updates the destination node via the wireless channel, are analysed in [28]. The authors consider a scenario where joint status sampling and updating process is designed to minimize the average AoI at the destination. The problem is formulated as an infinite horizon average cost constrained MDP that is transformed into an unconstrained MDP using a Lagrangian method. For the single IoT device, the optimal policy is shown to be of threshold type. Similar scenario is considered in [29], where an IoT device is classified as a secondary user that exploits the spectrum opportunities of the licensed band and updates the destination node.

Instead, the dimensionality problem in multi-source systems is tackled in [30], where the authors consider a multi-source RF-powered communication system and propose a reinforcement learning framework for optimizing the AoI.

B. Our Contributions

In this work, we consider a specific kind of multi-source system, where the status updates are generated upon request by an energy-harvesting *monitoring node* using multiple heterogeneous information *sources* that monitor the same underlying process. These different sources may capture different physical phenomena from an abstract perspective. For example, there may be multiple sensors monitoring the same process of interest using distinct technologies for the transducers, thus resulting in different accuracies and costs. Alternatively, the heterogeneity of the sources may stem from different channels that may convey the information (i.e., by means of different technologies, routes, communication links, or all of the above). Thus, each of the sources offers its own tradeoff of energy vs. age, resulting in information source diversity, and the monitoring node may seek to optimize the resulting AoI over time. This ought to take into account a constrained energy budget and the characteristics of all the information sources. In our model, each source may have available updates with different ages, due to its sampling of the underlying process at possibly diverse rates.

A sample scenario is crowdsensing, in which AoI can play an important role when choosing the source of updates. In crowdsensing, a monitor and some users are connected via the cloud [31]. The monitor sends the sensing task description to the users, and receives sensing plans, based on which to perform user selection. The AoI received from each information source depends on multiple factors such as sampling frequency, continuity of energy arrivals to the source nodes (assuming that the source nodes are powered by the ambient energy sources [32]), channel state, delay, and, in general, the robustness of a node.

Our first contribution is to analyze different heterogeneous information sources, and study how the combinations of cost and age distribution affect the resulting average AoI. We investigate the behavior of the optimal solution, which depends on the configuration of the information sources, through numerical analysis. In contrast to previous results in the literature [27]–[29], [33], we show through examples that the optimal policy exhibits a threshold behavior only versus the

few papers are focused on the average AoI with multiple information sources. In [20], [21], authors consider a system where independent sources send status updates through a shared first-come-first-serve M/M/1 queue to a monitor, and find the region of feasible average status ages for two and multiple sources. Similarly, in [22], a system with n sources is considered to provide status updates to multiple servers via a common queue. The authors formulate an AoI minimization problem and propose online scheduling policies. In [23], a single source node transmits status updates of two types to multiple receivers. The authors determine the optimal stopping thresholds to individually and jointly optimize the average age of two-type updates at the receiver nodes. In [24], a multi-objective formulation is proposed for scheduling transmissions in a system with multiple information sources that monitor different processes. The objective is to balance the AoI of these different processes. Similarly, in [25], the AoI minimization problem is also formulated for a system with multiple information sources that monitor different processes, and a monitoring node that communicates with the information sources through orthogonal channels. The authors propose the policy that converts the scheduling problem into a bipartite matching problem between the sets of channels and sensors. In [26], the authors study the scenario where a base station updates many network users. New information is randomly generated, and the base station can serve at most one user for each transmission. A structural MDP scheduling algorithm and an index scheduling algorithms were introduced.

One of the main challenges of deriving age-optimal transmission policies using MDP-based formulation is the large size of the state space of the system. This problem has been extensively studied for single-source systems. One of the ways to tackle this challenge is by demonstrating the optimality of a threshold-policy. In [27], the authors study a real-time IoT-enabled monitoring system in which a source node is responsible for maintaining the freshness of information status at a destination node. The source node is powered by wireless energy transfer. The authors adopt an MDP approach and characterize the throughput-optimal policy. In [15], the authors study the average AoI in EH cognitive radio communications, where the secondary user, i.e., EH sensor, performs spectrum sensing and status updates in a way that minimizes the average AoI based on its energy availability and the availability of the primary spectrum. The problem is formulated as a partially observable Markov decision process, and the optimal sensing and updating policies are shown to have threshold structure. The structural properties of the optimal policy for a

181 AoI but in general not when the energy increases, since some-
 182 times it may be convenient to refrain from updating and instead
 183 cumulating energy for a later update from a more expensive
 184 source.

185 As another contribution, we compare the performance of the
 186 optimal and aggressive policies, and find the threshold of the
 187 EH rate in which it is reasonable to apply the aggressive policy.
 188 We evaluate the effect of an increase in the average system cost
 189 on the performance. Finally, we assess if an increase in the
 190 number of information sources affects the overall performance.

191 C. Organization of the Paper

192 The rest of this paper is organized as follows. In Section II,
 193 the system description, problem formulation, and solution
 194 approaches are introduced. Numerical results are presented in
 195 Section III, providing a comparison with an aggressive policy.
 196 The paper is concluded in Section IV, where possible further
 197 developments are also outlined.

198 II. SYSTEM MODEL AND PROBLEM FORMULATION

199 We focus on a communication system formed by a sin-
 200 gle energy-harvesting monitoring node and n heterogeneous
 201 information sources, all capable of measuring the status of
 202 an underlying process. The monitoring node can query any
 203 of these information sources to receive an update on the sta-
 204 tus of the underlying process. For example, these information
 205 sources may model sensors with different technologies mea-
 206 suring the same process. In this paper, we consider such a
 207 general scenario, that could be further detailed to a multi-
 208 sensor, multi-radio, or multi-transducer scenarios [34], [35].
 209 Time is divided into slots of equal length, and we assume that
 210 the monitoring node can query from only one of the sources in
 211 each time slot. The received status update becomes available
 212 at the beginning of the next time slot. We highlight two impor-
 213 tant dynamics at the monitoring node: 1) energy fluctuations
 214 and 2) the AoI. The objective is to minimize the average AoI
 215 at the monitoring node taking into account the time-varying
 216 energy budget.

217 We assume that the monitoring node is equipped with a
 218 rechargeable battery of finite capacity B , and can harvest
 219 energy from ambient sources. Fluctuations in the battery of the
 220 monitoring node are defined by two processes: 1) harvested
 221 energy in each time slot and 2) the energy consumption caused
 222 by the queries for a status update. Energy harvested over time
 223 is represented as an independent and identically distributed
 224 (i.i.d.) binary random process $\{e(t)\}_{t=1}^{\infty}$. At each time slot t
 225 the monitoring node receives $e(t) \in \{0, \bar{e}\}$ energy units, such
 226 that $P(e(t) = \bar{e}) = \lambda$.

227 The energy cost of requesting an update from source i ,
 228 $i \in [n] \triangleq \{1, 2, \dots, n\}$, is denoted by c_i , a collective value
 229 that reflects the energy consumption of the monitoring node
 230 to acquire an update from source i . This may include the cost
 231 of sending a request and receiving an update if the sources
 232 are remote sensors, or simply the cost of operating that sen-
 233 sor if they are local. For simplicity, we consider $c_i \in \mathbb{Z}^+$
 234 corresponding to integer multiples of a unit of energy.

The AoI at time t , denoted by $\delta(t)$, refers to the age 235
 of the most recent status update available at the monitor- 236
 ing node [36]. If a more recent update is not received, 237
 $\delta(t)$ is increased by 1 at each time slot. We assume that 238
 $\delta(t) \in [0, 1, \dots, \delta_{\max}]$, as any AoI beyond δ_{\max} has the same 239
 utility for the system, which reduces the dimensionality of the 240
 problem. 241

The status updates provided by the information sources are 242
 not necessarily *fresh*, i.e., with zero age. Due to various fac- 243
 tors, such as the sensing technology or the processing of the 244
 measurements, we assume that the status updates may have 245
 different ages when they arrive at the monitoring node. We 246
 consider probabilistic AoI for the updates received from each 247
 information source; that is, we assume that the source nodes 248
 provide status updates with ages within the interval $[\alpha, \beta]$ 249
 ($\alpha < \beta$), where α is the most *fresh* status update while β is 250
 the most *stale* one, typically with different distributions. We 251
 assume that $\alpha \geq 1$, in order to incorporate the transmission 252
 time of the status update. 253

To model the different AoI distributions from each source, 254
 denote by $\gamma_{i,j}$ the probability of receiving a status update of 255
 age j from source i , where $j \in [\alpha, \beta]$ and $i \in [n]$. 256

It is reasonable to assume that the sources with higher prob- 257
 ability to deliver a fresh status update have a higher energy 258
 cost. Otherwise, a source which is both more costly and pro- 259
 vides more stale state updates would never be used, and can 260
 safely be removed from the system model. 261

A. Markov Decision Process (MDP) Formulation 262

We aim to determine the policy that minimizes the average 263
 AoI at the monitoring node. To achieve this, the monitoring 264
 node optimally chooses the action to take at each time slot. 265
 Possible actions include requesting an update from one of the 266
 information sources at the beginning of each time slot, or stay- 267
 ing idle. This choice is made taking into account the battery 268
 level and the age of the most recent status update available at 269
 the monitoring node. This problem can be formulated as an 270
 MDP, consisting of a tuple $\langle \mathcal{S}, \mathcal{A}, P, R \rangle$, where: 271

- \mathcal{S} is the state space where the process evolves; 272
- \mathcal{A} is the set of actions to control the state dynamics; 273
- P denotes the state transition probability function; 274
- R is the reward function defined on state transitions. 275

The action taken by the monitoring node at time t is 276
 denoted by $a(t)$, chosen from a finite action space $\mathcal{A} =$ 277
 $\{a_0, a_1, a_2, \dots, a_n\}$, where a_i corresponds to querying source 278
 i for an update, $i \in [n]$, while a_0 corresponds to remaining idle. 279
 The system state is described by the pair of variables $s(t) =$ 280
 $(b(t), \delta(t))$, $\delta(t) \in [\delta_{\max}]$ and $b(t) \in [B] \triangleq \{0, 1, \dots, B\}$. 281
 We denote by $\bar{\delta}(t)$ the age of the status update received at 282
 time t . Note that $\bar{\delta}(t)$ is a random variable depending on action 283
 $a(t)$. We set $\bar{\delta}(t) = \delta_{\max}$ if $a(t) = a_0$. Moreover, if $\bar{\delta}(t)$ hap- 284
 pens to be larger than the age of the already available status 285
 information, $\delta(t-1) + 1$, the current value is kept and no 286
 update is performed. Thus, the AoI is updated as: 287

$$\delta(t) = \min\{\delta(t-1) + 1, \bar{\delta}(t), \delta_{\max}\}. \quad (1) \quad 288$$

The energy level in the battery $b(t)$ at time t evolves according 289
 to the cost of an action taken and the harvested energy within 290

291 that time slot:

$$292 \quad b(t) = \min \left\{ b(t-1) - \sum_{i=1}^n c_i \cdot \mathbb{1}(a(t) = a_i) + e(t), B \right\},$$

293 (2)

294 where $\mathbb{1}(x)$ is the indicator function: $\mathbb{1}(x) = 1$ when x
 295 holds, and $\mathbb{1}(x) = 0$ otherwise. Action a_i is not allowed if
 296 $b(t) < c_i$, $i \in [n]$. We have a finite state space of dimension
 297 $\delta_{\max} \cdot (B + 1)$.

298 The transition probabilities are given below for $a_i \in$
 299 $\{a_1, a_2, \dots, a_n\}$, and $\delta(t) \in \{\alpha, \alpha + 1, \dots, \beta\}$.

$$300 \quad \begin{cases} P[s(t+1) = (\min\{b + \bar{e} - c_i, B\}, \min\{j, \delta + 1, \delta_{\max}\}) \\ |s(t) = (b, \delta), a(t) = a_i] = \lambda \gamma_{i,j} \text{ for } b \geq c_i, j \in [\alpha, \beta], \\ P[s(t+1) = (b - c_i, \min\{j, \delta + 1, \delta_{\max}\}) \\ |s(t) = (b, \delta), a(t) = a_i] = (1 - \lambda) \gamma_{i,j} \\ \text{for } b \geq c_i, j \in [\alpha, \beta], \end{cases}$$

301 (3)

302 When the node stays idle, i.e., $a(t) = a_0$, the transition
 303 probabilities take the following form:

$$304 \quad \begin{aligned} P[s(t+1) = (b, \min\{\delta + 1, \delta_{\max}\}) \\ |s(t) = (b, \delta), a(t) = a_0] &= 1 - \lambda \quad b < B \\ 305 \quad P[s(t+1) = (\min\{b + \bar{e}, B\}, \min\{\delta + 1, \delta_{\max}\}) \\ |s(t) = (b, \delta), a(t) = a_0] &= \lambda \quad b < B \\ 306 \quad P[s(t+1) = (B, \min\{\delta + 1, \delta_{\max}\}) \\ |s(t) = (B, \delta), a(t) = a_0] &= 1 \end{aligned}$$

307 (4)

310 Note that when the monitoring node chooses to stay idle and
 311 its energy storage is full (i.e., $B = b$), the state transition only
 312 involves the increase in the AoI since no more energy can be
 313 stored in the battery, therefore this transition is deterministic.
 314 The reward received at time t depends on the action chosen
 315 and the age of the update received at the monitoring node:

$$316 \quad R(s(t+1)|s(t), a(t) = a_i) = \delta(t+1). \quad (5)$$

317 The problem is framed as a first-order Markovian dynamics
 318 as the next state depends only on the current state $s(t)$ and the
 319 current action $a(t)$.

320 The deterministic stationary policy $\pi : \mathcal{S} \rightarrow \mathcal{A}$ defines an
 321 action $a(t)$ at each time slot depending on the current state. A
 322 stationary policy π means that $\pi_t = \pi$ for all $t = 1, 2, \dots$;
 323 we let δ_t^π denote the sequence of AoI caused by policy π . The
 324 infinite-horizon time-average AoI, when policy π is employed,
 325 starting from initial state s_0 , is defined as [36]:

$$326 \quad V^\pi(s_0) = \limsup_{T \rightarrow \infty} \frac{1}{T} \mathbb{E} \left[\sum_{t=0}^T \delta^\pi(t) | s(0) = s_0 \right]. \quad (6)$$

327 A policy is *optimal* if it minimizes the infinite-horizon
 328 average AoI - $V^\pi(s)$:

$$329 \quad V(s) = \min_{\pi} V^\pi(s). \quad (7)$$

330 To solve this optimization, we can use the offline dynamic
 331 programming approach, which is a quite common methodol-
 332 ogy successfully used in other problems related to efficient
 333 exploitation of harvested energy [37] and can be solved via

Algorithm 1 Relative VI Algorithm

```

set  $v^0(s) = 0 \forall s \in \mathcal{S}$ 
set  $n = 1, \epsilon > 0$ 
set  $V^0(s) = 0 \forall s \in \mathcal{S}$ 
repeat
   $n \leftarrow n + 1$ 
  for all  $s \in \mathcal{S}$  do
     $v^n(s) = \min_{a \in \mathcal{A}} \sum_{s' \in \mathcal{S}} P(s'|s, a) [\delta(s'|s, a) + V^{n-1}(s')]$ 
   $V^n(s) = v^n(s) - v^n(s_0)$ 
  where  $s_0$  is a fixed state chosen arbitrarily
  end for
until  $sp(V^n - V^{n-1}) < \epsilon$ 
return  $\arg \min V(s)$ 

```

standard techniques such as Value Iteration [38]. In the offline 334
 approach, we model the state transition function based on the 335
 prior knowledge of the age statistics of the updates received 336
 from different sources, $\gamma_{i,j}$, and the environmental character- 337
 istics, λ . The solution represents the map of actions to be 338
 chosen in different states. 339

III. PERFORMANCE EVALUATION 340

We compare the effect of different cost combinations and 341
 cost-reliability dependencies on the performance of differ- 342
 ent policies. We consider the cost distribution of information 343
 sources, the age distribution of updates received from different 344
 sources, and the parameter of the EH process, λ . 345

To validate the optimal approach, we compare its 346
 performance with that of the aggressive policy, which requests 347
 a status update at each time slot from the most costly 348
 information source that its current battery state affords. The 349
 optimal solution is obtained via the value iteration (VI) algo- 350
 rithm described in [38], which we also provide in Algorithm 1 351
 for completeness. The optimal stationary deterministic policy 352
 obtained by Algorithm 1 specifies the decision rules that maps 353
 the current energy level and AoI to deterministic actions. 354

In Algorithm 1, $sp(V^n - V^{n-1}) < \epsilon$ is a stopping criterion, 355
 where $sp(V) \triangleq \max_{s \in \mathcal{S}} V(s) - \min_{s \in \mathcal{S}} V(s)$. We run the 356
 relative VI algorithm until the stopping criterion holds. At 357
 that moment the policy π achieves an average-cost AoI that is 358
 within $\epsilon \cdot 100\%$ of optimal. 359

A. Impact of Different Cost Functions 360

Since our model and formulation are fairly general, the 361
 cost of requesting an update may result from very different 362
 reasons (sampling, processing and/or communication costs). 363
 Therefore, it is difficult to provide precise cost values and 364
 their relation across sources. We assume that the energy cost 365
 of any source takes values between c_{\min} and c_{\max} , where 366
 $0 < c_{\min} < c_{\max} < B$. In this way, we guarantee that all the 367
 sources are available to the monitoring node to query a status 368
 update as long as there is sufficient energy in the battery. In 369
 particular, we set the values of $c_{\min} = 0.05B$, $c_{\max} = 0.95B$. 370

To evaluate the effect of different cost combinations of the 371
 sources, we consider three cases, as per Fig. 2, each with the 372

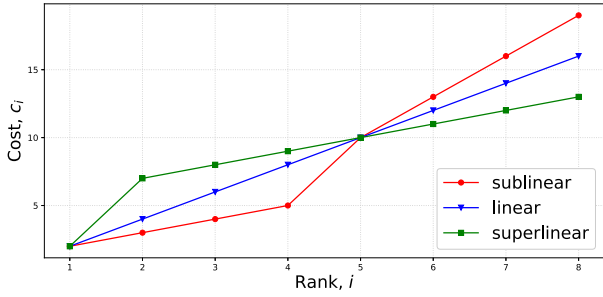


Fig. 2. Rank-cost dependencies.

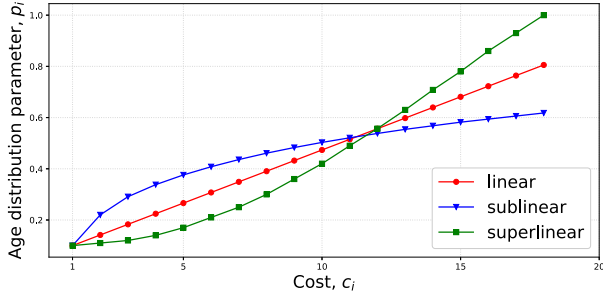


Fig. 3. Cost-age distribution dependency for the sublinear cost scenario.

373 same average cost value: *superlinear*, *linear* and *sublinear*. In
 374 Fig. 2, term ‘Rank’ corresponds to the index of source i , such
 375 that a source with a higher index has a higher rank and higher
 376 cost, respectively. The aforementioned dependencies do not
 377 carry any special “physical meaning”, they are simply chosen
 378 to investigate the impact of cost values on the average AoI.
 379 Indeed, other functions can also be used. Obviously, changing
 380 the average cost will affect the average AoI, but the effect of
 381 concavity on the target metric is not obvious. Thus, we focus
 382 on these trends to analyse the effect of “concavity” on the
 383 average AoI and also for easier reproducibility of our results.

384 B. Impact of Different Cost-Reliability Dependencies

385 Further, we evaluate the impact of different functions
 386 describing the cost-reliability dependencies. Similar with the
 387 cost function, in order to be able to perform a comparison we
 388 limit our attention to a specific class of age distributions from
 389 the sources. In particular, in our numerical analysis we assume
 390 that, for each i , $\gamma_{i,j}$ follows a geometric distribution with a
 391 different parameter p_i , as illustrated in Fig. 4. This model
 392 also allows us to parametrize the distributions with a single
 393 parameter. Hence, the distribution of the age of the received
 394 status update, when the i -th information source is chosen, is
 395 given by:

$$\begin{aligned}
 396 \quad \gamma_{i,j} &= Pr(\bar{\delta}(t) = j) = (1 - p_i)^{j-1} p_i, \\
 397 \quad & j = 1, 2, 3, \dots, \beta - 1
 \end{aligned} \quad (8)$$

398 Since we consider that packets with age higher than δ_{\max}
 399 have the same utility, we limit the geometric distribution to
 400 δ_{\max} . Additionally, $\gamma_{i,\beta} = Pr(\bar{\delta}(t) = \beta) = 1 - \sum_{j=1}^{\beta-1} (1 -$
 401 $p_i)^{j-1} p_i$ for every i . As stated earlier, we expect to receive
 402 more fresh status updates from a more costly source, at least on

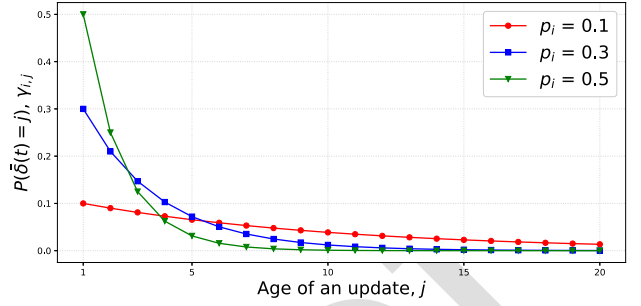

 Fig. 4. Geometric distribution of status updates for different p_i parameters, where $\bar{\delta}(t) \in [1, 20]$.

 TABLE I
 DEFAULT SYSTEM PARAMETERS

Parameters	Values
Battery capacity, B	20
AoI values of received updates, $[\alpha, \beta]$	$[1, 20]$
Amount of harvested energy per time slot, $\{0, \bar{e}\}$	$\{0, 3\}$
Number of sources, n	8
Cost range, $[c_{\min}, c_{\max}]$	$[1, 19]$
Maximum AoI, δ_{\max}	30

average. To quantify such a relation, we consider the following
 general functional choices to relate $p_i \in [0, 1]$ with c_i (Fig. 3):

$$\text{Sublinear: } p_i = k_{sub} \cdot c_i^2, \quad (9)$$

$$\text{Linear: } p_i = k_{lin} \cdot c_i, \quad (10)$$

$$\text{Superlinear: } p_i = k_{sup} \cdot \log_2 c_i, \quad (11)$$

where k_{sub} , k_{lin} , and k_{sup} are chosen such that the average
 system parameters of age distribution ($p = \gamma_i$) is the same, i.e.,
 $\frac{1}{n} \sum_{i=1}^n p_i$ is equal for the sublinear, linear and superlinear
 scenarios.

Once again, we would like to emphasize that our model and
 solution tools apply to arbitrary cost and age distributions, and
 these choices are made just to be able to observe the impact
 of three possible dependencies on the performance.

C. Results

Default system parameters common to all the simula-
 tions are presented in Table I. The efficiency of the optimal
 and aggressive policies is verified via simulation runs over
 $T = 5000$ time slots, averaged over $M = 1000$ simulations.
 To demonstrate the results we plot the AoI averaged over all
 times $t = \bar{1}, \bar{T}$.

The optimal solutions for different values of EH rates
 and cost-age distribution combinations are presented in
 Figs. 5 and 6. Both figures show the 9 possible combina-
 tions of cost and age distribution each taking values denoted
 by superlinear, linear, sublinear as in (9)–(11), see also
 Figs. 2 and 3.

We set $\lambda = 0.2$ in Fig. 5 and $\lambda = 0.6$ in Fig. 6. Each of
 the 9 subfigures shows the optimal policy depending on the
 system state. In both cases, $n = 8$ sources are considered, so
 the optimal policy chooses among 9 possible actions including
 “no update” (i.e., to stay idle).

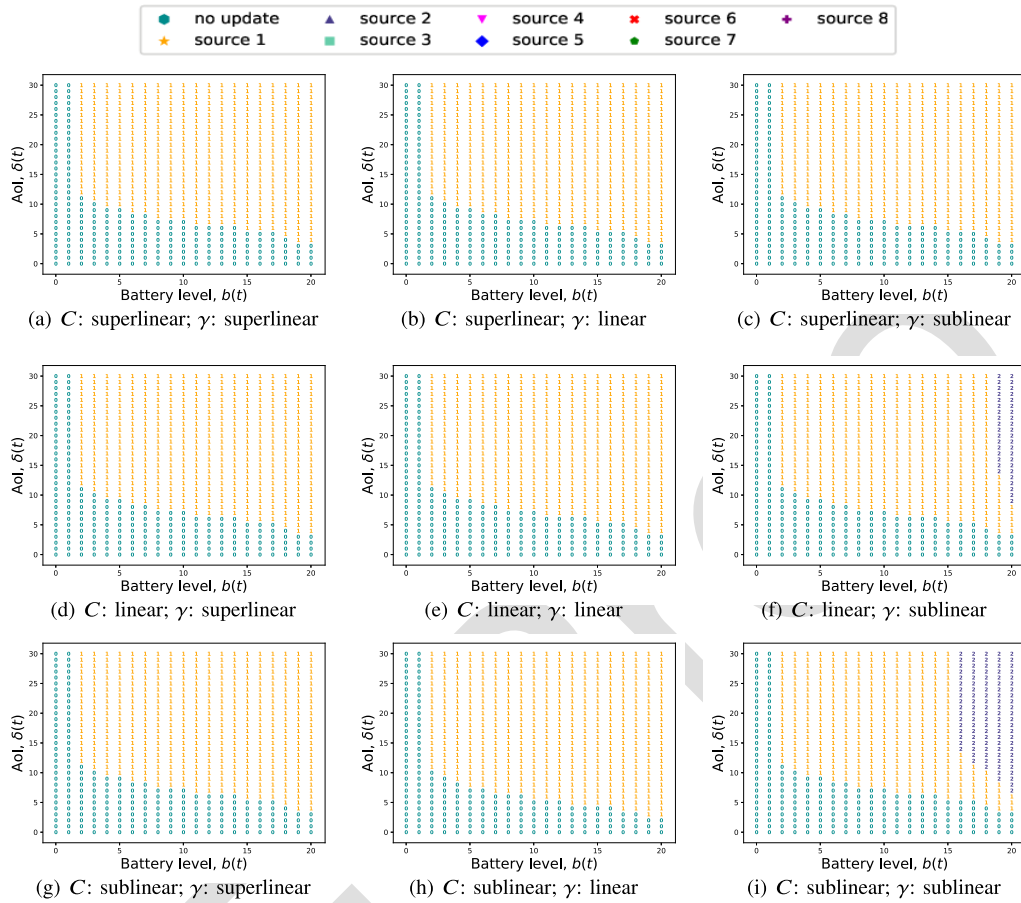


Fig. 5. Illustration of the optimal policy for different energy cost/ age distribution combinations for EH rate $\lambda = 0.2$.

Fig. 5 shows that when the EH rate is low, i.e., $\lambda = 0.2$, the monitoring node requests a status update only from the cheapest sources, i.e., sources 1, 2. Notably, the result is similar for all the combinations of cost and age distributions. In particular, the *activity region*, i.e., the set of states in which the monitoring node is actively requesting updates, remains the same. The activity region requires that both battery level and AoI are high enough to request an update.

For low values of AoI, the monitoring node never requests a status update, since the information is still fresh. Also, for low values of the battery level a status update cannot be afforded. However, differently from the aggressive approach, where an update is always requested if there is enough energy in the battery, the optimal policy, in contrast, conserves energy if the AoI is sufficiently low. This leads to an *energy saving region* for $\delta(t) \in [0, \delta_u(b(t))]$, where $\delta_u(b(t))$ is the highest AoI value for which no update is requested. The value of $\delta_u(b(t))$ decreases with $b(t)$, because at high battery levels the monitoring node can be more relaxed in status update requests. This trend applies for all cost-age distribution combinations in the same way. The only difference appears when the dependency of the parameters of the age distribution is sublinear, due to the fact that the more expensive source 2 is significantly more reliable, and therefore, worth using at higher energy levels. However, this also depends on the cost of source 2; if the cost dependence is also sublinear then

source 2 is employed instead of source 1 for lower values of $b(t)$.

The common aspect of all the 9 subplots in Fig. 5 is that only cheap sources are used when the energy arrivals are scarce. In contrast, Fig. 6 shows more variations in the usage of different sources for $\lambda = 0.6$. Here, similarly to Fig. 5, the same 9 cases are considered in the respective subfigures. For $\lambda = 0.6$, multiple sources are used depending not only on the values of $b(t)$ and $\delta(t)$, but also on the cost and age distribution combinations. Even though the *activity region* is approximately the same, it is split differently among multiple sources, and not necessarily only the cheapest ones. In particular, the baseline case where cost and dependency of age distribution parameters are both linear [Fig. 6(e)] demonstrates that a wide array of sources from 1 to 5 (i.e., the 5 cheapest ones) are used. The higher $b(t)$ and/or $\delta(t)$, the higher the index of the source used for the update.

If we change the cost from superlinear to sublinear [Figs. 6(b), 6(e), 6(h)], we see that, within the *activity region*, source 1 is used more or less consistently in all the 3 cases, but the patterns if other sources change, with intermediate sources becoming more widely used if the cost is sublinear. This trend is generally true if we read the subfigures from top to bottom. Based on the structural difference of the optimal solutions, the choice of the specific function is less important compared to its characteristics in terms of concavity/convexity.

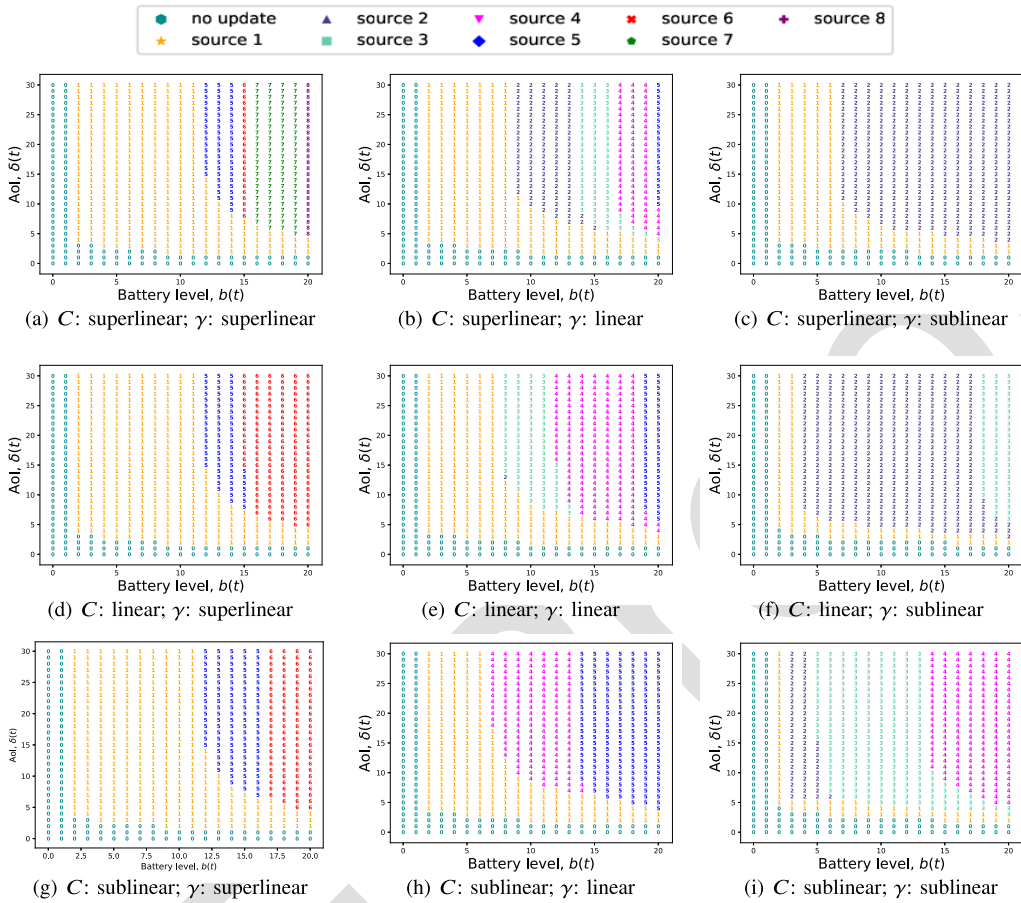


Fig. 6. Illustration of the optimal policy for different energy cost/ age distribution combinations for EH rate $\lambda = 0.6$.

Conversely, if we change the dependency of age distribution parameters [Figs. 6(d), 6(e), 6(f)], the cheaper sources are used more often, and their usage happens at lower battery levels, i.e., their region shifts towards left. This trend is also generally true if we read the subfigures from left to right.

D. Discussion

In this section, we prove some structural property of the optimal policy, in particular, an existence of a threshold effect on the battery level b (but notably, not on δ).

Theorem 1: If the AoI is unlimited (or, its maximum value is sufficiently high) then the optimal policy has an AoI-threshold-based behavior that holds for any value of b .

This means that if we focus on a given b , the optimal policy depends on the AoI δ such that:

- a given subset of $k(b)$ sources is used, denoted by $\sigma_1(b), \sigma_2(b), \dots, \sigma_{k(b)}(b) \in [N]$,
- exactly $k(b)$ threshold values for the AoI δ , denoted by $\vartheta_1(b), \vartheta_2(b), \dots, \vartheta_{k(b)}(b)$ can be defined, in strictly increasing order (i.e., $\vartheta_j(b) < \vartheta_{j+1}(b)$ for every $j \in [N-1]$), so that source $\sigma_j(b)$ is used only when $\vartheta_j(b) \leq \delta < \vartheta_{j+1}(b)$ for $j \in [N-1]$, and the last source $\sigma_{k(b)}(b)$ is used for $\delta \geq \vartheta_{k(b)}(b)$, while no update is attempted if $\delta < \vartheta_1(b)$.

This threshold-based character of the optimal policy under the aforementioned conditions, can be proven through the following two lemmas.

Lemma 1: A system with $n \geq 2$ sources has an optimal AoI-threshold-based activation $\vartheta_1(b)$ for all values of e , meaning the optimal policy is to stay idle (action a_0) when $\delta < \vartheta_1(b)$, and conversely action a_0 is suboptimal if $\delta \geq \vartheta_1(b)$.

Proof: The details are reported in Appendix A. ■

Following this Lemma, one can see that if $\delta \geq \vartheta_1(b)$ it is convenient to update but it is not known from which source. We need to obtain a full AoI-threshold-based structure as required by the theorem to show that, if a given b is considered and δ is increased from $\vartheta_1(b)$, there are other turning points $\vartheta_2(b), \vartheta_3(b), \dots$ such that for $\delta \geq \vartheta_j(b)$ the optimal action switches from $s_j(b)$ to $s_{j+1}(b)$ and never reverts back to $s_j(b)$ after that point. This is shown through this last Lemma.

Lemma 2: Consider a given value of b and two different sources i and j , whose associated update actions are a_i and a_j , respectively. If a_i is preferable over a_j when the battery level is b and the AoI value is δ_1 , where $\delta_1 \geq \vartheta_1(b)$, and the reverse happens (i.e., a_j is preferable over a_i) for battery level b and AoI equal to $\delta_2 > \delta_1$, then a_j is necessarily better than a_i for battery level b and all AoI values $\delta > \delta_2$.

The proof is provided in Appendix B. We remark that the theorem proves an AoI-threshold-based behavior, but in general we do not have a similar behavior in the battery level b , as discussed in the following counterexample.

Counterexample: Consider a scenario with two information sources, where $\delta_{\max} = 1$, and $\alpha = 0$ $\beta = 1$. The two

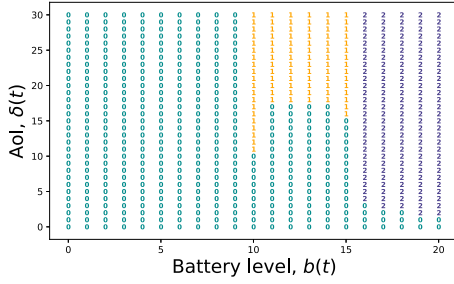


Fig. 7. Optimal solution ($p_2 = 1$, $p_1 = 0.1$, $\lambda = 0.9$).

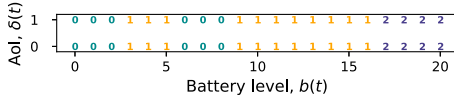


Fig. 8. Optimal solution: $N = 1$, $p_2 = 0.99$, $c_1 = 5$, $c_2 = 11$, $\lambda = 0.9$, $\bar{e} = 5$.

information sources 1 and 2 have the following characteristics:
 $0 < c_1 < c_2 < B$, $p_2 \gg p_1$.

Compare the time-average AoI for $T = 2$ for the following sequences of actions performed by the monitoring node:

Sequence 1: (use 1; use 1), resulting in $\bar{\delta} = 1 - p_1 + \frac{(1-p_1)^2}{2}$.
Sequence 2: (do not transmit; use 2), resulting in $\bar{\delta} = 1 + \frac{1-p_2}{2}$.

If $p_2 > 4p_1 - p_1^2$, then sequence 2 is preferable over sequence 1. However, sequence 2 may not be available if using source 2 is too expensive for the current battery state. In other words, depending on the current energy state and energy arrivals, it may be more convenient to just use the cheap source or to wait in order to enable the expensive source in the subsequent time slot. Formally, this happens if $b(0) - c_1 + \lambda h > c_2$. Hence, we proved that with an increase in the state of the battery at time 0, the minimization of AoI can imply to use a cheaper source at time 1 (in this specific example, no source at all), which contradicts the monotonicity of the source index in the battery level.

In Fig. 8, we demonstrate the effect of limiting N on the structure of the optimal solution. We considered a system with two sources with $p_1 = 0.2$, $p_2 = 0.99$, $c_1 = 5$, $c_2 = 11$. The AoI distribution is kept geometric in range $[\alpha, \beta] = [0, 20]$. The energy-harvesting process is given with parameters $\lambda = 0.9$, $\bar{e} = 5$. We observe the energy saving region that occurs under this particular combination of parameters.

Another visual counterexample is also graphically presented in Fig. 7, where we adopt the default settings from Table I, and consider two sources such that $p_2 \gg p_1$, $\lambda = 0.9$. We also increased the value of parameter \bar{e} so that the energy buffer can recover fast. The costs of sources are set as follows $c_1 = 1$, $c_2 = 16$. The distribution of AoI is preserved as geometric in range $[\alpha, \beta] = [1, 20]$. In this setup, the optimal policy is not threshold-based with respect to the battery level.

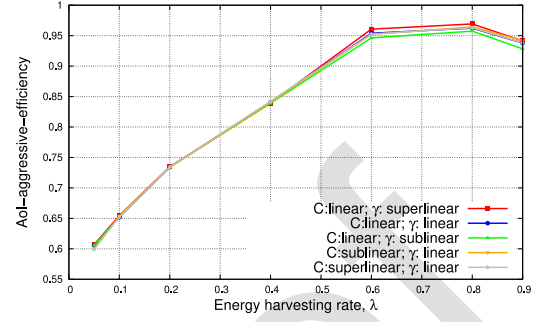


Fig. 9. Rate between the average AoI obtained by the optimal and aggressive policies as a function of the EH rate.

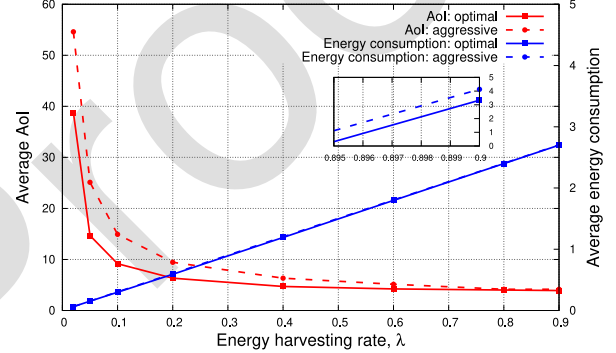
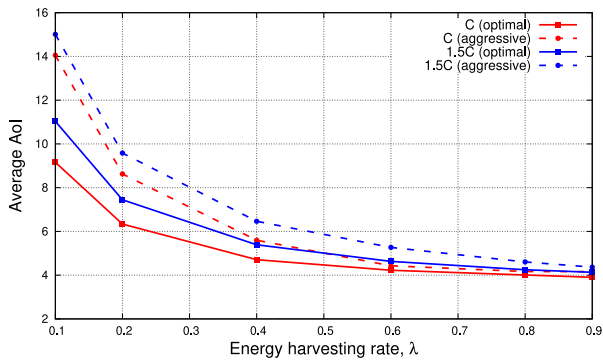
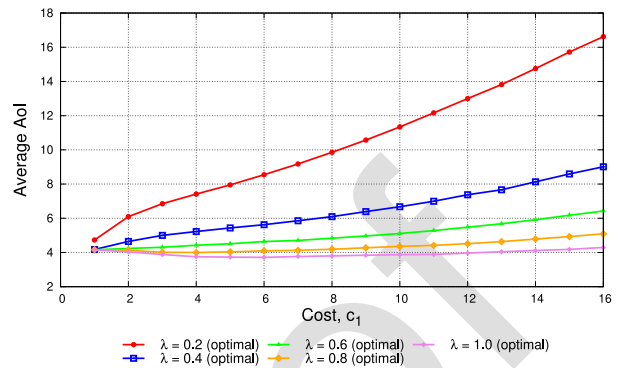


Fig. 10. EH rate, λ vs average AoI and average energy consumption.

E. Performance Comparison

To understand the potential benefits of the optimal policy, we compare it with the aggressive policy as a benchmark. In Fig. 9 we plot the relative gain over the aggressive policy vs the EH rate λ , where the AoI-aggressive-efficiency in the y-axis is defined as the ratio between the average AoI obtained by the optimal strategy to the one obtained by the aggressive policy. For the sake of brevity, five cost and age distribution combinations are considered. High (close to 1) AoI-aggressive-efficiency implies that the aggressive policy is quite efficient, and benefit of using the more computationally demanding VI framework is limited. Despite some differences in the structure of the optimal solution, the resulting AoI-aggressive-efficiency has similar values for all cost-age distribution combinations. The AoI-efficiency-rate increases with λ , meaning that the difference in performance between optimal and aggressive policy vanishes at high λ . In particular, for $\lambda > 0.5$ the AoI-aggressive-efficiency saturates above 0.90. We can conclude, that if the energy arrivals are relatively stable, the benefits of optimization is rather limited. On the other hand, for low values of λ the optimization of the update policy is much more relevant, which follows the intuition. Yet, when λ is very low, the role of multiple sources is minimal, and only the cheapest sources are used (see Fig. 5).

In Fig. 10, we plot the average AoI and the average energy consumption vs. the EH rate. As one would expect, the average energy consumption increases with λ , while the average AoI decreases. We observe that the two policies have almost identical energy consumption, for low λ values, although the optimal policy provides significantly lower average AoI performance.

Fig. 11. EH rate, λ , vs average AoI for linear cost-age distribution.Fig. 12. Optimal average AoI vs. cost of an information source for different values EH rates, λ .

605 Also, the energy consumption of the aggressive policy saturates at high λ values, while that of the optimal policy continues to increase linearly.

608 We also analyzed the average AoI when the average update cost is 50% higher than the default case. To do so, we increased the cost of each source 1.5 times (1.5C) and found the average AoI for the linear cost-age distribution case, as demonstrated in Fig. 11. With the increase of cost, the difference between the average AoI achieved by the optimal and aggressive policies reaches up to 15%, if λ is low. When λ is high, the difference in performance is insignificant.

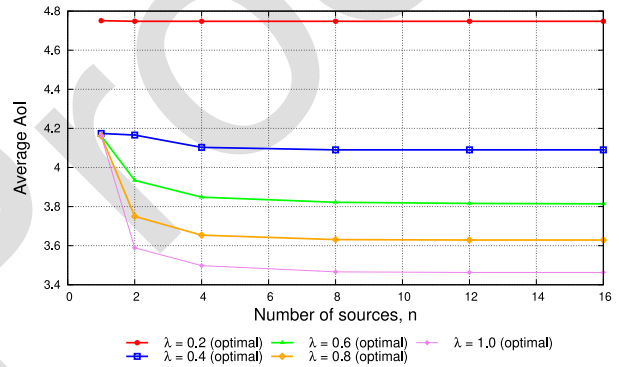
616 F. Network Size

617 Further, we analyze how the number n of information sources affects the performance for different values of EH rate, λ , and energy arrival units, \bar{e} . The analysis is performed for linear scaling of the costs of the devices, and a linear dependency between the cost and the number of the sources.

622 We decrease the space of actions (or network size) in the following manner: first, we form the vector of size n with costs $[c_1, c_2, \dots, c_n]$, and derive the average AoI for n information sources. Then, we reduce the network size by half at each step till we have only two information sources with cost vector $[c_1, c_n]$, thus we obtain the average AoI for $n = 2, 4, 8, 16$. For $n = 12$, we randomly removed four sources.

629 Firstly, we consider a system without sources diversity, i.e., with a single information source; and demonstrate the dependency of optimal average AoI and cost of that source. With the increase in the cost, the optimal average AoI increases, despite the fact that with the increase of the cost, the probability to receive a fresh status update increases. Moreover, in the greatest extent, an increase in cost affects the performance in case of low frequency energy arrivals (see Fig. 12). If the cost value is low, i.e., $c_1 = 1$, the performance for different values of λ has minor variation. In particular, the performance is identical if λ is sufficiently high ($\lambda \geq 0.4$). Although, when $\lambda = 0.2$ the optimal solution has a larger energy saving area, which is why we observe a larger gap in performance.

642 With the increase in the number of information sources, the optimal average AoI has a tendency to decrease, but the curves eventually saturate when the number of sources reaches $n = 8$ (Fig. 13). The largest gain in performance is obtained when the system is of size $n = 2$. If the EH rate is low ($\lambda = 0.2$

Fig. 13. Optimal average AoI vs. number of information sources for different values of EH rates, λ .

in Fig. 13), then the increase in the number of devices does not provide any gain for the system performance, but with an increase in the EH rate, the gain increases as the system size goes from $n = 1$ to $n = 2$ if $\lambda \leq 0.6$. If $\lambda \geq 0.4$ the gain obtained by an increase of the system size from $n = 1$ to $n = 2$ and from $n = 2$ to $n = 4$ is similar. Nevertheless, in the performance comparison in case of $n = 1$ we consider the best performing setting, i.e., $c_1 = 1$, $p_1 = 0.1$. If $c_1 > 1$, $p_1 > 0.1$, the gain is much more significant when the system size is increased from $n = 1$ to $n = 2$. A similar statement holds true when we vary the values of energy arrivals, \bar{e} . This is because, when the EH rate is low, the monitoring node almost exclusively uses the “cheaper” information sources, so introducing more expensive alternatives does not help.

661 If the monitoring node exploits the aggressive strategy, then we observe a counterintuitive behaviour: with an increase in the system size for $n > 2$, the performance worsens, or, in other words, the average AoI at the monitoring node increases. Moreover, the lower λ , the higher the increase in the average AoI, or the more inefficient the aggressive policy becomes. This effect is particularly negative for low λ values because the aggressive policy always goes for the most expensive information source it can afford. Introducing more expensive alternatives means that they will end up being used rather than the cheaper sources. This results in a poorer performance particularly for low λ values, when it is optimal to exploit only the cheapest sources. Yet, when $\lambda \geq 0.4$ introducing system diversity slightly improves the performance;

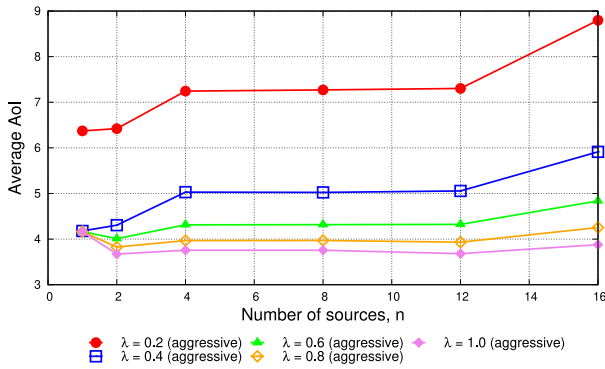


Fig. 14. Average AoI vs. number of information sources vs. if the monitoring node adopts aggressive strategy for different values of the EH rate, λ .

675 actually, the best performance is provided by $c_1 = 8$ (see
 676 Fig. 12), therefore, when we shift from $C = [1]$ to $C = [16, 1]$
 677 we achieve the “balance” and an improvement in the
 678 performance. However, with a further increase of the system
 679 size the “balance” shifts causing an increase in average AoI
 680 (see Fig. 14).

681 IV. CONCLUSION

682 In this work, we considered a system model with a sin-
 683 gle energy-harvesting monitoring node that can request status
 684 updates from multiple heterogeneous information sources that
 685 monitor the same process of interest. We assumed that the
 686 energy cost of requesting an update, as well as the statistics
 687 of the age of the received update varies across the information
 688 sources. In order to analyze the system, we considered dif-
 689 ferent combinations of costs and age distributions that are
 690 described in detail in Section III.

691 We formulated the long-term average AoI minimization
 692 problem as an MDP, and obtained the optimal solution using
 693 the relative VI algorithm. We then studied the optimal solu-
 694 tion for different EH rates and found out that the solutions
 695 are more sensitive to the age distribution rather than the
 696 costs of the status updates. We demonstrated that having
 697 just the cheapest sources is mostly sufficient if the EH
 698 rate is low. We also considered an aggressive policy, which
 699 requests a status update from the most expensive source it
 700 can afford at each time slot, as a benchmark. We observed
 701 that the aggressive policy is near optimal when the EH rate
 702 is high.

703 We found that adding information sources beyond a cer-
 704 tain number does not help, particularly if the available sources
 705 already provide sufficient diversity in terms of the cost-average
 706 age trade-off within the available energy sources.

707 Future work includes an extended model comprising the
 708 channel dynamics and the resulting transmission time and
 709 costs, as well as more general EH schemes [39]. Another
 710 direction is to study reinforcement learning to choose the
 711 information source to use over time without depending on the
 712 explicit information on the age distributions of the sources or
 713 the statistics of the EH process [30].

APPENDIX A PROOF OF LEMMA 1

714 The lemma requires to prove, for any b , the existence of a
 715 $\vartheta_1(b)$ such that it is convenient to update if and only if $\delta \geq$
 716 $\vartheta_1(b)$. First of all, for $b < b_0 = \min_{j=1,2,\dots,N} c_j$, then the
 717 statement is trivially true with an infinite $\vartheta_1(b)$ as all sources
 718 are too expensive to update.
 719

720 Define $\bar{R}(s(t) = (b, \delta), a_i)$ as the average optimal reward
 721 starting from the current state $s(t) = (b, \delta)$ and after taking
 722 action $a(t) = a_i$. According to our model, if $i > 0$, that is,
 723 we perform an actual update from source i , we evolve to a
 724 state with either energy level $b - c_i$ or $b - c_i + \bar{e}$ (depending
 725 on the EH process) and AoI $\epsilon \in \mathcal{E}_i = [\alpha, \min(\beta, \delta + 1)]$ with
 726 probability $\tilde{\gamma}_i(\epsilon)$, which is defined as follows. If $\beta \leq \delta$ then
 727 $\tilde{\gamma}_i(\epsilon) = \gamma_i(\epsilon)$ for all ϵ . If $\beta > \delta$ then $\tilde{\gamma}_i(\epsilon) = \gamma_i(\epsilon)$ for $\epsilon \in [\alpha, \delta]$
 728 and $\tilde{\gamma}_i(\delta + 1) = \sum_{n=\delta+1}^{\beta} \gamma_i(n)$.
 729

730 From (4) and (5) we can write the following Bellman
 731 equation for $\bar{R}(s(t), a_i)$ being

$$\begin{aligned} \max_{j \in \Omega} \left[(1 - \lambda) \sum_{\epsilon \in \mathcal{E}_i} (\epsilon + \tilde{\gamma}_i(\epsilon) \bar{R}(s(t+1) = (b - c_i, \epsilon), a_j)) \right. \\ \left. + \lambda \sum_{\epsilon \in \mathcal{E}_i} (\epsilon + \tilde{\gamma}_i(\epsilon) \bar{R}(s(t+1) = (b - c_i + \bar{e}, \epsilon), a_j)) \right], \end{aligned} \quad (12)$$

where $\Omega = \{0, \dots, n\}$

732 Given that ϵ does not depend on a_j , (12) can be written as:

$$\begin{aligned} (1 - \lambda) \sum_{\epsilon \in \mathcal{E}_i} \left(\epsilon + \tilde{\gamma}_i(\epsilon) \max_{j \in \Omega} \bar{R}(s(t+1) = (b - c_i, \epsilon), a_j) \right) \\ + \lambda \sum_{\epsilon \in \mathcal{E}_i} \left(\epsilon + \tilde{\gamma}_i(\epsilon) \max_{j \in \Omega} \bar{R}(s(t+1) = (b - c_i + \bar{e}, \epsilon), a_j) \right) \end{aligned} \quad (13)$$

733 whereas if we do not update (action a_0) we obtain

$$\begin{aligned} \bar{R}(s(t), a_0) = (1 - \lambda) \\ \times \left(\delta + \max_{j \in \Omega} \bar{R}(s(t+1) = (b, \delta + 1), a_j) \right) \\ + \lambda \left(\delta + \max_{j \in \Omega} \bar{R}(s(t+1) = (b + \bar{e}, \delta + 1), a_j) \right) \end{aligned} \quad (14)$$

744 We notice that (13) is not explicitly influenced by δ , which
 745 is incidentally logical as, after the update, δ is reset to a “low”
 746 AoI value,¹ whereas (14) is increasing in δ . This implies that as
 747 δ increases, there exists a turning point $\vartheta_1(b)$ that makes (13)
 748 smaller than (14) and this stays true for all values of $\delta \geq$
 749 $\vartheta_1(b)$.

APPENDIX B PROOF OF LEMMA 2

750 Similarly to the previous lemma, we can compare the
 751 Bellman equations for the updates from two different sources

¹To be precise, the set \mathcal{E}_i actually depends on δ but only for the reason
 that whenever the update is supposed to be to a value in $[\alpha, \beta]$ that is higher
 than $\delta + 1$, the update information is actually useless and discarded, see (1).

i and j . Note that we are always considering AoI values $\delta > \vartheta_1(b)$ for which an update is preferable to staying idle, as proven in Lemma 1. And since we are updating in both cases, we lose any explicit dependence on the AoI δ , as per (13) - in other words, after either update action, the system trajectory evolves from states with “low” AoI. Finally, we remark that $\bar{R}((b, \delta), a)$ is always non-decreasing in δ for given b and action a . This implies that if $\bar{R}((b, \delta_1), a_i) < \bar{R}((b, \delta_1), a_j)$ but $\bar{R}((b, \delta_2), a_i) > \bar{R}((b, \delta_2), a_j)$, then $\bar{R}((b, \delta), a_i) > \bar{R}((b, \delta), a_j)$ also for every $\delta > \delta_2$; that is, a source to update from can be the optimal one only over a set of contiguous AoI values.

REFERENCES

- [1] E. Gindullina, L. Badia, and D. Gündüz, “Average age-of-information with a backup information source,” in *Proc. IEEE 30th Annu. Int. Symp. Pers. Indoor Mobile Radio Commun. (PIMRC)*, Istanbul, Turkey, 2019, pp. 1–6.
- [2] F. Javed, M. K. Afzal, M. Sharif, and B.-S. Kim, “Internet of Things (IoT) operating systems support, networking technologies, applications, and challenges: A comparative review,” *IEEE Commun. Surveys Tuts.*, vol. 20, no. 3, pp. 2062–2100, 3rd Quart., 2018.
- [3] S. Kaul, R. Yates, and M. Gruteser, “Real-time status: How often should one update?” in *Proc. IEEE INFOCOM*, Orlando, FL, USA, 2012, pp. 2731–2735.
- [4] S. Kaul, M. Gruteser, V. Rai, and J. Kenney, “Minimizing age of information in vehicular networks,” in *Proc. 8th Annu. IEEE Commun. Soc. Conf. Sens. Mesh Ad Hoc Commun. Netw. (SECON)*, Salt Lake City, UT, USA, 2011, pp. 350–358.
- [5] Q. Zhang and F. H. P. Fitzek, “Mission critical IoT communication in 5G,” in *Future Access Enablers of Ubiquitous and Intelligent Infrastructures*. Cham, Switzerland: Springer, 2015, pp. 35–41.
- [6] D. Gunduz, K. Stamatiou, N. Michelusi, and M. Zorzi, “Designing intelligent energy harvesting communication systems,” *IEEE Commun. Mag.*, vol. 52, no. 1, pp. 210–216, Jan. 2014.
- [7] E. T. Ceran, D. Gündüz, and A. György, “Reinforcement learning to minimize age of information with an energy harvesting sensor with HARQ and sensing cost,” in *Proc. IEEE Conf. Comput. Commun. Workshops (INFOCOM WKSHPS)*, Paris, France, 2019, pp. 656–661.
- [8] X. Wu, J. Yang, and J. Wu, “Optimal status update for age of information minimization with an energy harvesting source,” *IEEE Trans. Cogn. Commun. Netw.*, vol. 2, no. 1, pp. 193–204, Mar. 2018.
- [9] A. Arafa, J. Yang, S. Ulukus, and H. V. Poor, “Age-minimal transmission for energy harvesting sensors with finite batteries: Online policies,” *IEEE Trans. Inf. Theory*, vol. 66, no. 1, pp. 534–556, Jan. 2020.
- [10] A. Arafa, J. Yang, and S. Ulukus, “Age-minimal online policies for energy harvesting sensors with random battery recharges,” in *Proc. IEEE Int. Conf. Commun. (ICC)*, Kansas City, MO, USA, 2018, pp. 1–6.
- [11] B. T. Bacinoglu, Y. Sun, E. Uysal, and V. Mutlu, “Optimal status updating with a finite-battery energy harvesting source,” *J. Commun. Netw.*, vol. 21, no. 3, pp. 280–294, Jun. 2019.
- [12] M. Dabiri and M. J. Emadi, “Average age of information minimization in an energy harvesting wireless sensor node,” in *Proc. 9th Int. Symp. Telecommun. (IST)*, Tehran, Iran, 2018, pp. 123–126.
- [13] S. Feng and J. Yang, “Age of information minimization for an energy harvesting source with updating erasures: Without and with feedback,” *IEEE Trans. Commun.*, early access, May 26, 2021, doi: 10.1109/TCOMM.2021.3083803.
- [14] B. T. Bacinoglu, Y. Sun, E. Uysal-Bivikoglu, and V. Mutlu, “Achieving the age-energy tradeoff with a finite-battery energy harvesting source,” in *Proc. IEEE Int. Symp. Inf. Theory (ISIT)*, Vail, CO, USA, 2018, pp. 876–880.
- [15] S. Leng and A. Yener, “Age of information minimization for an energy harvesting cognitive radio,” *IEEE Trans. Cogn. Commun. Netw.*, vol. 5, no. 2, pp. 427–439, Jun. 2019.
- [16] S. Feng and J. Yang, “Minimizing age of information for an energy harvesting source with updating failures,” in *Proc. IEEE Int. Symp. Inf. Theory (ISIT)*, Vail, CO, USA, 2018, pp. 2431–2435.
- [17] S. Farazi, A. G. Klein, and D. R. Brown, “Average age of information for status update systems with an energy harvesting server,” in *Proc. IEEE Conf. Comput. Commun. Workshops (INFOCOM WKSHPS)*, Honolulu, HI, USA, 2018, pp. 112–117.
- [18] S. Farazi, A. G. Klein, and D. R. Brown, “Age of information in energy harvesting status update systems: When to preempt in service?” in *Proc. IEEE Int. Symp. Inf. Theory (ISIT)*, Vail, CO, USA, 2018, pp. 2436–2440.
- [19] A. Arafa, J. Yang, S. Ulukus, and H. V. Poor, “Online timely status updates with erasures for energy harvesting sensors,” in *Proc. Allerton Conf. Commun. Control Comput.*, 2018, pp. 966–972.
- [20] R. D. Yates and S. K. Kaul, “The age of information: Real-time status updating by multiple sources,” *IEEE Trans. Inf. Theory*, vol. 65, no. 3, pp. 1807–1827, Mar. 2019.
- [21] R. D. Yates and S. Kaul, “Real-time status updating: Multiple sources,” in *Proc. IEEE Int. Symp. Inf. Theory (ISIT)*, Cambridge, MA, USA, 2012, pp. 2666–2670.
- [22] Y. Sun, E. Uysal-Biyikoglu, and S. Kompella, “Age-optimal updates of multiple information flows,” in *Proc. IEEE Conf. Comput. Commun. Workshops (INFOCOM WKSHPS)*, Honolulu, HI, USA, 2018, pp. 136–141.
- [23] B. Buyukates, A. Soysal, and S. Ulukus, “Age of information in multicast networks with multiple update streams,” in *Proc. 53rd Asilomar Conf. Signals Syst. Comput.*, Pacific Grove, CA, USA, 2019, pp. 1977–1981.
- [24] N. Pappas, J. Gunnarsson, L. Kratz, M. Kountouris, and V. Angelakis, “Age of information of multiple sources with queue management,” in *Proc. IEEE Int. Conf. Commun. (ICC)*, London, U.K., 2015, pp. 5935–5940.
- [25] V. Tripathi and S. Moharir, “Age of information in multi-source systems,” in *Proc. IEEE Global Commun. Conf.*, Singapore, 2017, pp. 1–6.
- [26] Y.-P. Hsu, E. Modiano, and L. Duan, “Scheduling algorithms for minimizing age of information in wireless broadcast networks with random arrivals,” *IEEE Trans. Mobile Comput.*, vol. 19, no. 12, pp. 2903–2915, Dec. 2020.
- [27] M. A. Abd-Elmagid, H. S. Dhillon, and N. Pappas, “Online age-minimal sampling policy for RF-powered IoT networks,” in *Proc. IEEE Global Commun. Conf. (GLOBECOM)*, Waikoloa, HI, USA, 2019, pp. 1–6.
- [28] B. Zhou and W. Saad, “Joint status sampling and updating for minimizing age of information in the Internet of Things,” *IEEE Trans. Commun.*, vol. 67, no. 11, pp. 7468–7482, Nov. 2019.
- [29] Q. Wang, H. Chen, Y. Gu, Y. Li, and B. Vucetic, “Minimizing the age of information of cognitive radio-based IoT systems under a collision constraint,” *IEEE Trans. Wireless Commun.*, vol. 19, no. 12, pp. 8054–8067, Dec. 2020.
- [30] M. A. Abd-Elmagid, H. S. Dhillon, and N. Pappas, “A reinforcement learning framework for optimizing age of information in RF-powered communication systems,” *IEEE Trans. Commun.*, vol. 68, no. 8, pp. 4747–4760, Aug. 2020.
- [31] D. Yang, G. Xue, X. Fang, and J. Tang, “Incentive mechanisms for crowdsensing: Crowdsourcing with smartphones,” *IEEE/ACM Trans. Netw.*, vol. 24, no. 3, pp. 1732–1744, Jun. 2016.
- [32] D. Altinel and G. K. Kurt, “Modeling of multiple energy sources for hybrid energy harvesting IoT systems,” *IEEE Internet Things*, vol. 6, no. 6, pp. 10846–10854, Dec. 2019.
- [33] S. Leng and A. Yener, “Minimizing age of information for an energy harvesting cognitive radio,” in *Proc. IEEE Wireless Commun. Netw. Conf. (WCNC)*, Marrakesh, Morocco, 2019, pp. 1–6.
- [34] N. Himayat *et al.*, “Multi-radio heterogeneous networks: Architectures and performance,” in *Proc. IEEE Int. Conf. Comput. Netw. Commun. (ICNC)*, Honolulu, HI, USA, 2014, pp. 252–258.
- [35] T. Qiu, N. Chen, K. Li, M. Atiquzzaman, and W. Zhao, “How can heterogeneous Internet of Things build our future: A survey,” *IEEE Commun. Surveys Tuts.*, vol. 20, no. 3, pp. 2011–2027, 3rd Quart., 2018.
- [36] E. T. Ceran, D. Gündüz, and A. György, “Average age of information with hybrid ARQ under a resource constraint,” *IEEE Trans. Wireless Commun.*, vol. 18, no. 3, pp. 1900–1913, Mar. 2019.
- [37] I. Fawaz, M. Sarkiss, and P. Ciblat, “Optimal resource scheduling for energy harvesting communications under strict delay constraint,” in *Proc. IEEE Int. Conf. Commun. (ICC)*, Kansas City, MO, USA, 2018, pp. 1–6.
- [38] M. L. Puterman, *Markov Decision Processes: Discrete Stochastic Dynamic Programming*. New York, NY, USA: Wiley, 2014.
- [39] S. Priya and D. J. Inman, *Energy Harvesting Technologies*, vol. 21. New York, NY, USA: Springer, 2009.



897 **Elvina Gindullina** received the M.S. degree (Hons.)
 898 in applied mathematics and computer science from
 899 Ufa State Aviation Technical University (USATU),
 900 Russia, in 2015, and the Ph.D. degree in information
 901 and communication technologies from University
 902 of Padua (UNIPD), Italy, in 2020. From 2014 to
 903 2016, she was a Programmer with USATU. In
 904 2016, she moved to UNIPD. In 2016, she joined
 905 SCAVENGE Project (Horizon 2020) as an Early
 906 Stage Researcher, under the Marie Skłodowska-
 907 Curie Actions programme, where she was working
 908 on battery management systems, energy cooperation solutions and increas-
 909 ing of energy efficiency for energy harvesting IoT networks. In 2018, she
 910 conducted her internship with Worldensing, Barcelona, Spain, as a Research
 911 Engineer, where she was designing sampling strategies for an industrial data-
 912 logger powered by a solar panel. She is currently a Research Assistant with
 913 the Department of Information Engineering, UNIPD, where she is developing
 914 and analysing the novel models and methods for effective connectivity in a
 915 whole-brain network.



916 **Leonardo Badia** (Senior Member, IEEE) received
 917 the Laurea degree (Hons.) in electrical engineer-
 918 ing and the Ph.D. degree in information engineer-
 919 ing from the University of Ferrara, Italy, in 2000
 920 and 2004, respectively. From 2002 to 2003, he
 921 was on leave from the Radio System Technology
 922 Labs (currently, Wireless@KTH), Royal Institute
 923 of Technology, Stockholm, Sweden. After having
 924 been with the Engineering Department, University
 925 of Ferrara, he joined in 2006 the IMT Institute for
 926 Advanced Studies, Lucca, Italy. In 2011, he moved
 927 to the University of Padua, Italy, where he is currently an Associate Professor.
 928 He published more than 140 research papers. He is involved in the coordina-
 929 tion of scientific events and projects. His research interests include protocol
 930 design for multihop networks, cross-layer optimization of wireless commu-
 931 nication, transmission protocol modeling, and applications of game theory to
 932 radio resource management. He is also an active referee of research articles,
 933 having served on the editorial boards and still being an active reviewer for
 934 many scientific periodicals, as well as technical program committee chair for
 935 conferences in the broad area of networking and wireless communications.



936 **Deniz Gündüz** (Senior Member, IEEE) received the
 937 M.S. and Ph.D. degrees in electrical engineering
 938 from NYU Tandon School of Engineering (formerly,
 939 Polytechnic University) in 2004 and 2007, respec-
 940 tively. After the Ph.D., he served as a Postdoctoral
 941 Research Associate with Princeton University, and
 942 as a Consulting Assistant Professor with Stanford
 943 University. From September 2009 until September
 944 2012, he served as a Research Associate with
 945 CTTC, Barcelona, Spain. In September 2012, he
 946 joined the Electrical and Electronic Engineering
 947 Department, Imperial College London, U.K., where he is currently a Professor
 948 of Information Processing, serves as the Deputy Head of the Intelligent
 949 Systems and Networks Group, and leads the Information Processing and
 950 Communications Laboratory. He is also a part-time Faculty Member with
 951 the University of Modena and Reggio Emilia, and has held visiting posi-
 952 tions with University of Padova from 2018 to 2020, and Princeton University
 953 from 2009 to 2012. His research interests lie in the areas of communications
 954 and information theory, machine learning, and privacy. He is an Area Editor
 955 of the IEEE TRANSACTIONS ON COMMUNICATIONS and IEEE JOURNAL
 956 ON SELECTED AREAS IN COMMUNICATIONS—Special Series on Machine
 957 Learning in Communications and Networks. He also serves as an Editor of
 958 the IEEE TRANSACTIONS ON WIRELESS COMMUNICATIONS.